# The Enhancement of $^{226}$Ra in a Tidal Estuary due to the Operation of Fertilizer Factories and Redissolution from Sediments: Experimental Results and a Modelling Study

**R. Periáñez**

*Dpto. Física Aplicada I., Universidad de Sevilla, Ingeniería Técnica Agrícola, Ctra. Utrera km 1, 41013-Sevilla, Spain. e-mail: perianez@cica.es*

The presence of $^{226}$Ra in a tidal estuary formerly affected by direct discharges from a phosphate fertilizer complex has been investigated. In general, activity levels are lower than those detected when direct discharges were carried out. However, there is still a clear contamination that can be attributed, presumably, to the disposal of Ra-containing phosphogypsum to the river and to the redissolution of radionuclides from the contaminated sediments. A numerical model of the estuary has been developed to investigate these hypothesis. The hydrodynamics are first calibrated and standard tidal analysis is carried out. The dispersion model computes instantaneous currents from the so obtained tidal constants to speed up simulations. The exchanges of $^{226}$Ra between water and the bottom sediment have been described in terms of kinetic transfer coefficients. Model results are, in general, in agreement with observations. The simulation results support the previous idea of sediments acting as a source of $^{226}$Ra to the water column.

**Keywords:** $^{226}$Ra; fertilizer; phosphogypsum; sediment; redissolution; tides; numerical model; dispersion; Huelva estuary

## Introduction

Fertilizers containing phosphate have become essential to agriculture. They are used to replenish natural nutrients removed from the soil because of farming and erosion. It is well known that the phosphate rock used for fertilizer production contains significant amounts of natural radionuclides, mostly U, Th and Ra. Such content depends on the geographical origin of the rock but, generally speaking, ranges from 50 to 300 ppm (Laiche & Scott, 1991). The industrial processing of phosphate rock leads to some redistribution of radioactivity. It is known, for instance, that during the wet process (Guimond & Hardin, 1989) for phosphoric acid production, 86% of U and 70% of Th present in the rock appear in the phosphoric acid itself, while 80% of the Ra content follows the so-called phosphogypsum. This is a form of impure calcium sulfate removed as a precipitate during the process. Phosphogypsum is usually disposed into piles in the open environment or discharged into rivers or estuaries, giving rise to a clear local radioactive impact.

The Huelva estuary is located at the southwest of Spain. It consists of a tidal, fully mixed, estuary formed by the Odiel and Tinto rivers, which surround the town of Huelva (Figure 1). Both rivers join at the Punta del Sebo. From this point, they flow together through the same channel towards the Atlantic Ocean. A phosphate fertilizer processing complex located by the Odiel river has released wastes directly to the Odiel waters. Thus, anomalously high activity levels of $^{226}$Ra, U- and Th-isotopes have been detected in waters and sediments collected from the estuary (Periáñez & García-León, 1993; Martínez-Aguirre *et al.*, 1994; Periáñez & Martínez-Aguirre, 1997). However, the waste policy of the fertilizer complex has changed due to new regulations from the EU. Thus, wastes are not discharged directly into the Odiel river, although phosphogypsum is still being disposed in piles at the open air by the Tinto river (see Figure 1).

The objective of this work consists of studying the effect of the new waste policy on the presence of $^{226}$Ra in waters of the Odiel and Tinto rivers. This can give information on the cleaning processes of contaminated estuaries (not only by radioactive elements, but by chemicals in general) that can be useful not only at a local scale, but in general for estuarine environments with similar characteristics.

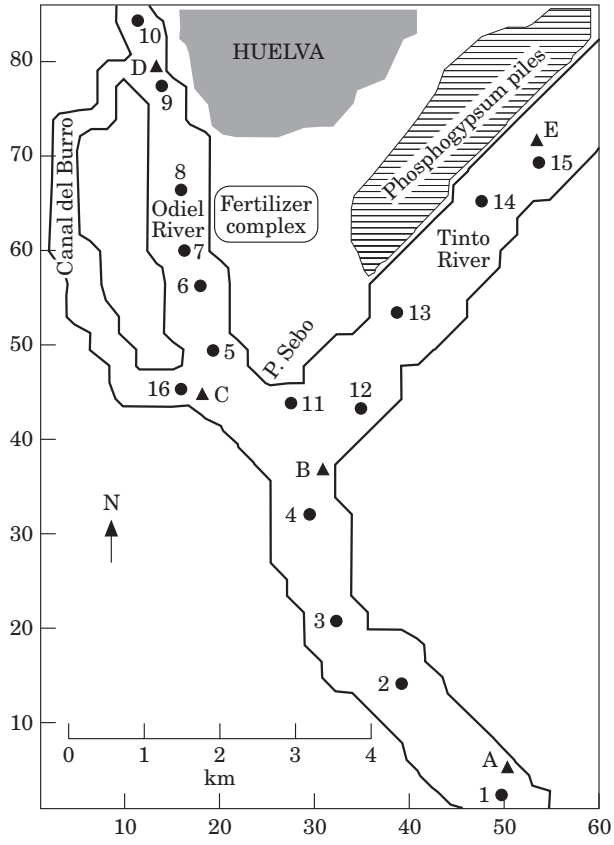


FIGURE 1. Map of the area of the estuary covered by the model. Numbered circles indicate the points where water samples were collected. Lettered triangles indicate the points where currents measurements were available. Units on the axes give the grid cell number. The sea is approximately 1 km to the south of point 1.

Water samples were collected and $^{226}$Ra activities determined. The interpretation of the experimental results is not an easy task. Thus, a numerical model of the estuary has been developed. The model solves the hydrodynamics of the estuary and the dispersion of $^{226}$Ra, including the interactions between the dissolved and solid (bottom sediments) phases.

In the next section, the sampling and experimental methods are described. Next, experimental results are discussed. Finally, the modelling work is presented.

## Experimental

Water samples were collected along the Odiel and Tinto rivers in October 1999. The sampling points, numbered from 1 to 16, are shown in Figure 1. A ship moving along the rivers was used for sampling. Sampling of the Tinto river (samples 11 to 15) plus points five and 16 was carried out during low water (11:00h, local time). Samples one to four were collected approximately 2 h later and samples six to 10 approximately 4 h later. These delays, due to the time required by the ship to travel, are important in the context of the modelling work. At three points of the estuary (5, 9 and 12), samples were also collected at different times along the tidal cycle to investigate the influence of the tidal state on the activity levels.

Samples were collected in 25 l plastic bottles, and pH was measured at the same time. The water was filtered soon after sampling, using Nuclepore filters 0·45 μm pore size, so as to remove suspended particles, and acidified to pH 2–3 with $HNO_3$ to avoid the growth of microorganisms and minimize water-wall interactions during storage.

$^{226}$Ra activities were determined from 0·5 l of water sample. For that, the water was neutralized with $NH_4OH$. Then some 5 mg of $BaCl_2$ was dissolved in it and about 20 ml of 1 m $H_2SO_4$ was added to the water. $RaSO_4$ coprecipitates with $BaSO_4$ under these conditions after some 20 min of continuous stirring. The sample was then filtered through Millipore filters, 0·45 μm pore size. Activity from the filter is measured using a LB770 low background gas flow proportional counter previously calibrated for total efficiency vs precipitate mass thickness.

These procedures have been widely validated and applied. More details can be seen, for instance, in Morón *et al.* (1986), Martínez-Aguirre *et al.* (1991) and Periáñez and García-León (1993).

## Experimental results

$^{226}$Ra activities and pH of waters are presented in Table 1. Activities range from 3·6 to 46 mBq $l^{-1}$ and are, in general, similar to those detected in other rivers affected by the discharge of wastes from fertilizer plants, as is the case of Boben river (Kobal *et al.*, 1990) and the Schelde estuary (Koster *et al.*, 1992), in Slovenia and the Netherlands respectively. In the first case 43 mBq $l^{-1}$ of $^{226}$Ra were measured; in the second, activities ranged from 9 to 68 mBq $l^{-1}$. However, activities in the estuary are, in general, lower than those detected when direct discharges were carried out to the Odiel river: some 7 to 670 mBq $l^{-1}$ (Periáñez & García-León, 1993).

It can be seen in Table 1 that the Tinto river (samples 12 to 15) is more contaminated than the Odiel river (samples 5–10 plus 16). This can be attributed to the phosphogypsum piles located by the Tinto river: they are crossed by a number of streams of natural and artificial origin that presumably are transporting Ra from the piles to the river. Although the pH values in the system are generally low, the lower pH of samples 13 and 15 reveals that some

TABLE 1. $^{226}$Ra activities (mBq l$^{-1}$) in water samples of the Odiel and Tinto rivers. Errors ($1\sigma$) are due to counting statistics in sample measurements and in detector calibration. NM means not measured. Hours are local times

| Station | Time | $A_{226}$ (mBq l) | pH |
|---|---|---|---|
| 1 | 13:00 | 3·6 ± 0·6 | 7 |
| 2 | 13:00 | 19·1 ± 1·5 | 5 |
| 3 | 13:00 | 16·4 ± 1·8 | 6 |
| 4 | 13:00 | 19·6 ± 2·1 | 5 |
| 5 | 11:00 | 16·4 ± 1·6 | 5 |
| 5 | 15:00 | 14·2 ± 0·7 | NM |
| 6 | 15:00 | 13·0 ± 0·6 | 6 |
| 7 | 15:00 | 17·9 ± 2·2 | 6 |
| 8 | 15:00 | 11·0 ± 0·6 | 5 |
| 9 | 13:15 | 9·9 ± 0·9 | NM |
| 9 | 15:00 | 11·3 ± 1·0 | 5 |
| 10 | 15:00 | 6·8 ± 0·6 | 5 |
| 11 | 11:00 | 15·9 ± 1·7 | 5 |
| 12 | 11:00 | 45 ± 5 | 5 |
| 12 | 12:55 | 46 ± 7 | NM |
| 12 | 15:05 | 23·2 ± 1·0 | NM |
| 12 | 17:00 | 19·1 ± 1·3 | NM |
| 13 | 11:00 | 35·3 ± 1·8 | 4 |
| 14 | 11:00 | 28·5 ± 4·1 | 5 |
| 15 | 11:00 | 25·1 ± 2·3 | 4 |
| 16 | 11:00 | 14·0 ± 0·9 | 6 |

external input is occurring. Before the change of the waste policy of the factory, the Odiel river was clearly more contaminated than the Odiel river (Periáñez & García-León, 1993).

In sample 1, collected close to the sea, activity decreases to 3·6 mBq l$^{-1}$, approaching to the average $^{226}$Ra content in Atlantic waters of 1·07 mBq l$^{-1}$ (Broeker *et al.*, 1976). The activity of sample 10 is lower than in the rest of the river due to the fact that this point is some kilometres upstream from the fertilizer complex and thus, remains relatively unaffected. Activity levels measured along the Odiel river (samples 5–9 plus 16) and in samples two to four are rather uniform. This contrasts with the situation when direct discharges were carried out: a clear activity peak could be detected close to the factory outlet (Periáñez & García-León, 1993). However, activity levels are still higher than those found in non-perturbed rivers. This activity enhancement in the Odiel river can be due to a redissolution of $^{226}$Ra from the contaminated river sediment. It is known that a certain amount of released radionuclides can be removed from the water column and incorporated to bottom sediments. However, these sediments cannot be considered as a final repository for radionuclides since, in fact, there is strong evidence (see Cook *et al.*, 1997 for instance) to suggest that the contaminated sediments become a source of re-mobilized radionuclides when the external input is reduced and desorption reaction dominates absorption. This hypothesis will be studied in more detail with the help of the numerical model described below.

It seems that there is not a clear dependence of activities at points five and nine upon the tidal state. This is not the case of the point 12, where activity during low tide is a factor two higher than activity during high tide (it should be noted, however, that only two samples are available for points five and nine, while four samples were collected in point 12). This suggests that $^{226}$Ra introduced into the Tinto river from the phosphogypsum piles moves downstream during the ebb, giving place to an activity peak that is detected downstream the piles during low water. During the flood, the input of relatively clean water reduces the activity levels. All these processes will also be studied with the help of the mathematical model.

## Model description

The system under study is divided into a number of grid cells or compartments. Two phases are present in each grid cell: dissolved and active bottom sediments (particles with a diameter <62·5 μm), as denoted by Benes *et al.* (1994). Thus, the active sediments correspond to muddy sediments, following the Wentworth scale of sediment grain size (see for instance Pugh, 1987). Larger grain sizes are not considered since it has been found (Aston *et al.*, 1985) that virtually all the radioactivity is associated with the muddy sediment. Also, a modelling study (Periáñez, 1999) has revealed that specific activity in the sandy component of the sediment can be neglected when compared with specific activity in the active sediment.

Suspended matter particles have not been considered in the model, and thus deposition processes and erosion of the sediment have been neglected. This approximation is used since previous calculations have shown that the radionuclide absorption capacity of suspended matter, given the typical suspended matter concentrations at the estuary, maximum concentrations of the order of 50 ppm (Periáñez *et al.*, 1996*b*), is very small compared with that of the sediment. Moreover, the erosion-deposition rates, obtained from a suspended matter model of the estuary (Periáñez *et al.*, 1996), are small (of the order of $10^{-2}$ g cm$^{-2}$ year$^{-1}$).Thus, as an approximation, it has been considered that the most important phases controlling radionuclide transport are the dissolved phase and the bottom sediment. This approximation seems realistic given the generally good agreement between model results and observations (see below).

Absorption and desorption reactions are described in terms of kinetic transfer coefficients (Nyffeler *et al.*, 1984). Thus, the absorption process (transfer of radionuclides from water to the sediment) will be governed by a coefficient $k_1$ and the inverse process (desorption to the dissolved phase) by a coefficient $k_2$. The absorption process is a surface phenomenon that depends on the surface of particles per water volume unit into the grid cell. This quantity has been denoted as the exchange surface (Periáñez *et al.*, 1996*a*; Periáñez, 1999, 2000). Thus:

$$k_1 = \chi_1 S \tag{1}$$

where $S$ is the exchange surface and $\chi_1$ is a parameter with the dimensions of a velocity. It is denoted as the exchange velocity (Periáñez *et al.*, 1996*a*).

As a first approach, assuming spherical sediment particles and a step function for the grain size distribution of particles, it can be obtained (Periáñez *et al.*, 1996*a*) that

$$S = \frac{3Lf\phi}{RH} \tag{2}$$

where $R$ is the mean radius of sediment particles, $H$ is the total water depth, $L$ is the average mixing depth (the distance to which the dissolved phase penetrates the sediment), $f$ gives the fraction of active sediment and $\phi$ is a correction factor that takes into account that not all the exchange surface of the sediment particle is in contact with water since part of it can be hidden by other particles. Thus, it is implicitly assumed that radionuclide concentration in pore waters of the sediment, into a sediment layer of thickness $L$ inside which the sediment is homogeneous, corresponds to concentration in the water column. On the other hand, diffusion of radionuclides to deeper sediment layers has been neglected given the time scale of the simulations that are carried out (Periáñez *et al.*, 1996*a*).

The transfer coefficient $k_2$ is considered constant. This description of the transfer of radionuclides between a dissolved and a solid phase has been used successfully in previous modelling studies (Periáñez, 1999, 2000).

Of course, dissolved radionuclides will be transported along the estuary by advective and diffusive process. Thus, the hydrodynamic equations must be solved too.

### *Hydrodynamics*

The 2D shallow water hydrodynamic equations are (see for instance Pugh, 1987):

TABLE 2. Observed and computed magnitude and direction of the maximum currents for a tide of coefficient 74·4. The orientation is measured anticlockwise from east. Points are shown in Figure 1

| Point | Computed | | Observed | |
|---|---|---|---|---|
| | Mag ($m\ s^{-1}$) | Direc (deg) | Mag ($m\ s^{-1}$) | Direc (deg) |
| A | 0·62 | 129·4 | 0·66 | 126·6 |
| B | 0·53 | 95·6 | 0·56 | 127·1 |
| C | 0·56 | 132·5 | 0·67 | 141·8 |
| D | 0·47 | 127·2 | 0·49 | 162·1 |
| E | 0·54 | 45·8 | 0·48 | 52·2 |

$$\frac{\partial z}{\partial t} + \frac{\partial}{\partial x}[(D+z)u] + \frac{\partial}{\partial y}[(D+z)v] = 0 \tag{3}$$

$$\frac{\partial u}{\partial t} + u\frac{\partial u}{\partial x} + v\frac{\partial u}{\partial y} + g\frac{\partial z}{\partial x} - \Omega v + K\frac{u\sqrt{u^2+v^2}}{D+z} = 0 \tag{4}$$

$$\frac{\partial v}{\partial t} + u\frac{\partial v}{\partial x} + v\frac{\partial v}{\partial y} + g\frac{\partial z}{\partial y} + \Omega u + K\frac{v\sqrt{u^2+v^2}}{D+z} = 0 \tag{5}$$

where $u$ and $v$ are the depth averaged water velocities along the $x$ and $y$ axis, $D$ is the depth of water below the mean sea level, $z$ is the displacement of the water surface above the mean sea level measured upwards, $\Omega$ is the Coriolis parameter ($\Omega = 2w\beta$, where $w$ is the earth rotational angular velocity and $\beta$ is latitude), $g$ is acceleration due to gravity and $K$ is the bed friction coefficient. The use of a 2D model is justified since the estuary is very shallow (maximum depth around 19 m) and well mixed in the vertical. Moreover, the stream flows of the rivers are very low (ranging from 4 to 50 $m^3\ s^{-1}$ in usual conditions) and a fast dispersion of fresh water into a much larger volume of salt water occurs (Borrego & Pendón, 1988). This mixing takes place upstream of the studied area, thus horizontal gradients of salinity are not considered.

The solution of these equations provide the instantaneous values of the two components of the current and the water elevation over the model domain, information required to solve the advection-diffusion dispersion equation of dissolved radionuclides.

### *Radionuclide equations*

The equation that gives the temporal evolution of specific activity in the dissolved phase, $C_d$ ($Bq\ m^{-3}$), is:

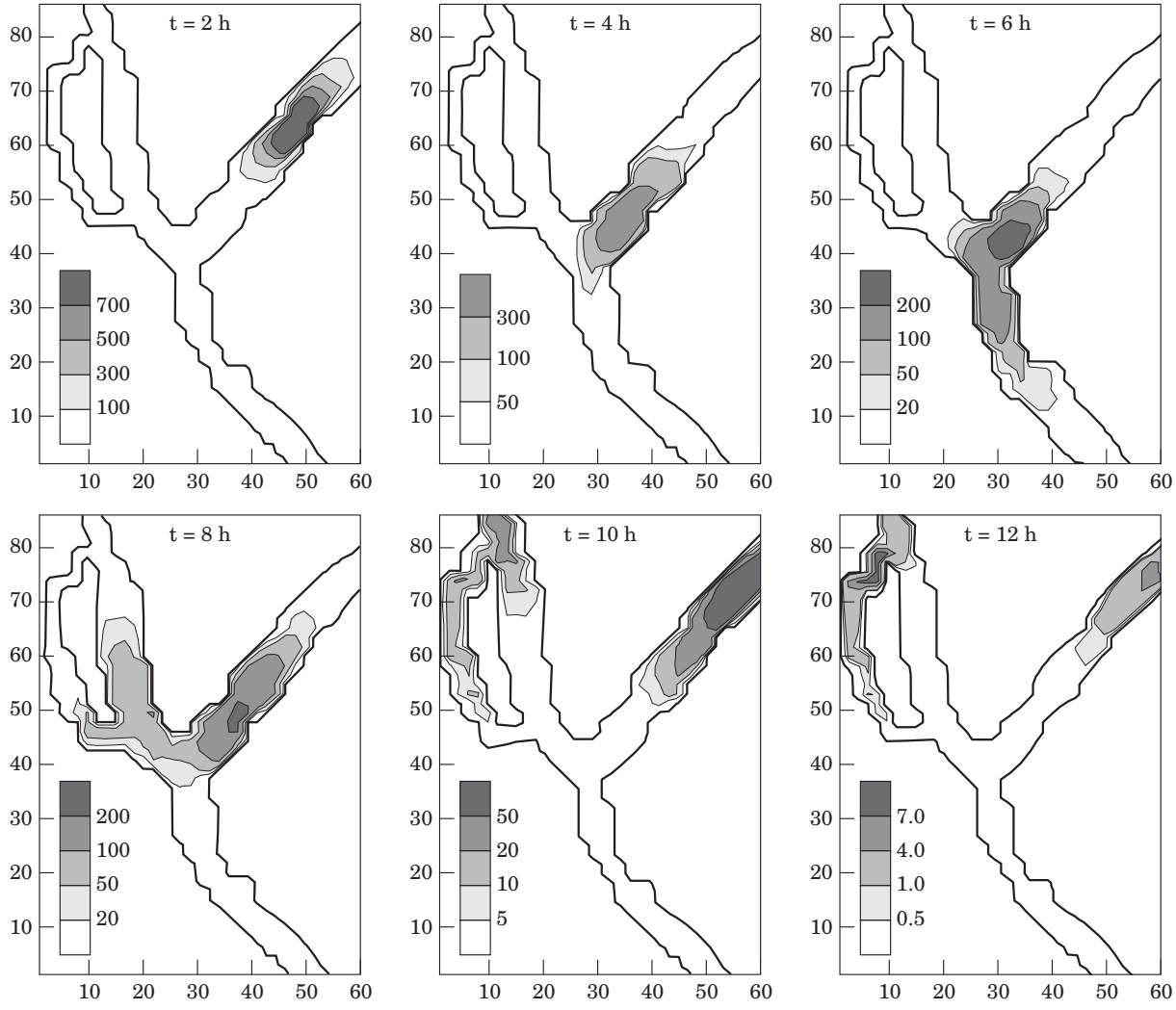


FIGURE 2. Time evolution of dissolved concentrations resulting after an activity input of arbitrary magnitude carried out in the Tinto river during high water.

$$\frac{\partial(HC_d)}{\partial t}+\frac{\partial(uHC_d)}{\partial x}+\frac{\partial(vHC_d)}{\partial y}=\frac{\partial}{\partial x}\left(HK_D\frac{\partial C_d}{\partial x}\right)+\frac{\partial}{\partial y}\left(HK_D\frac{\partial C_d}{\partial y}\right)-k_1C_dH+k_2A_sL\rho_sf\phi 10^3 \quad (6)$$

where $k_1$ is given by equations 1 and 2, total depth is $H=D+z$, $K_D$ is the diffusion coefficient, $A_s$ (Bq g$^{-1}$) is specific activity in the active sediment and $\rho_s$ is the sediment bulk density expressed in kg m$^{-3}$. The external source of radionuclides should be added to this equation in the points where it exists.

The equation for the temporal evolution of specific activity in the active sediment fraction is:

$$\frac{\partial A_s}{\partial t}=k_1\frac{C_dH}{L\rho_sf}10^{-3}-k_2A_s\phi \quad (7)$$

*Computational scheme*

The hydrodynamic equations are solved using the explicit finite difference scheme described in Flather and Heaps (1975). The grid cell size is $\Delta x=\Delta y=$ 125 m and time step is fixed as $\Delta t=6$ s. The CFL criterion is satisfied with these selections. Water elevations are specified for each time step along the southern boundary from observations (Puerto Autónomo de Huelva, 1989). A radiation condition (Kowalick & Murty, 1993) is applied along the northern and eastern open boundaries. Along the coast, the current component that is normal to the boundary is set to zero. Water depths were introduced for each grid cell from bathymetric maps.

Instead of solving the hydrodynamic equations simultaneously with the dispersion equations, the

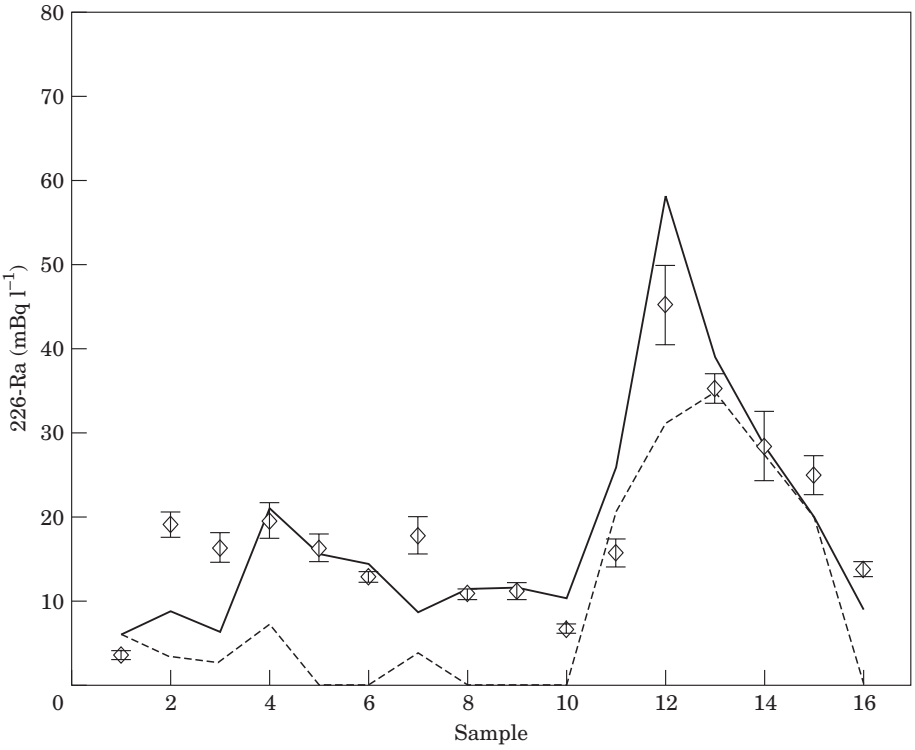


FIGURE 3. Comparison between observed and computed specific activities in water along the estuary. Model results when the sediments are not included in the computations are also shown. —— Computed; –◇– Measured; – – – No sediments.

hydrodynamic model is calibrated and validated in advance to speed up simulations. Once the hydrodynamics have been validated, standard tidal analysis is used to determine the tidal constants (amplitude and phase) for each grid cell. These constants are evaluated for both components of the flow ($u$ and $v$) and for the water elevation ($z$), and for all the tidal constituents included in the model. Once the tidal constants are know, computation of flow and water elevation just involves the calculation and addition of a few cosine terms since the constants are stored in files that are read by the dispersion model. The net residual flow over the estuary must also be calculated by the hydrodynamic model and added to the instantaneous flow obtained from the tidal constants, since a residual transport cannot be generated with the pure harmonic currents that are given by the tidal analysis.

The MSOU (Monotonic Second Order Upstream) explicit scheme (Vested *et al.*, 1996) is used to solve the advective transport in the dispersion equation of dissolved radionuclides. A few indications are given below (for simplicity, only the 1D formulation is shown): the advection equation

$$\frac{\partial C}{\partial t}+\frac{\partial (uC)}{\partial x}=0 \tag{8}$$

can be written in finite differences, on a fixed staggered computational grid, as:

$$\frac{C_j^{n+1}-C_j^n}{\Delta t}\Delta x = T_{j-1}^n - T_j^n \tag{9}$$

with

$$T_j^n = F_j^n u_j^n \tag{10}$$

The first order upwind scheme is obtained if $F_j^n = C_j^n$. In the MSOU:

$$F_j^n = C_j^n + \tfrac{1}{2}\psi_j \Delta C_j \tag{11}$$

where $\Delta C_j = C_j^n - C_{j-1}^n$ and

$$\psi_j = \max[0, \min(2r_j, 1), \min(r_j, 2)] \tag{12}$$

with

$$r_j = \frac{C_{j+1}^n - C_j^n}{C_j^n - C_{j-1}^n} \tag{13}$$

This is valid in the case of flow in the positive direction. The space index must be switched if the flow is in the opposite direction. Details can be seen in Vested *et al.* (1996). A second order accuracy

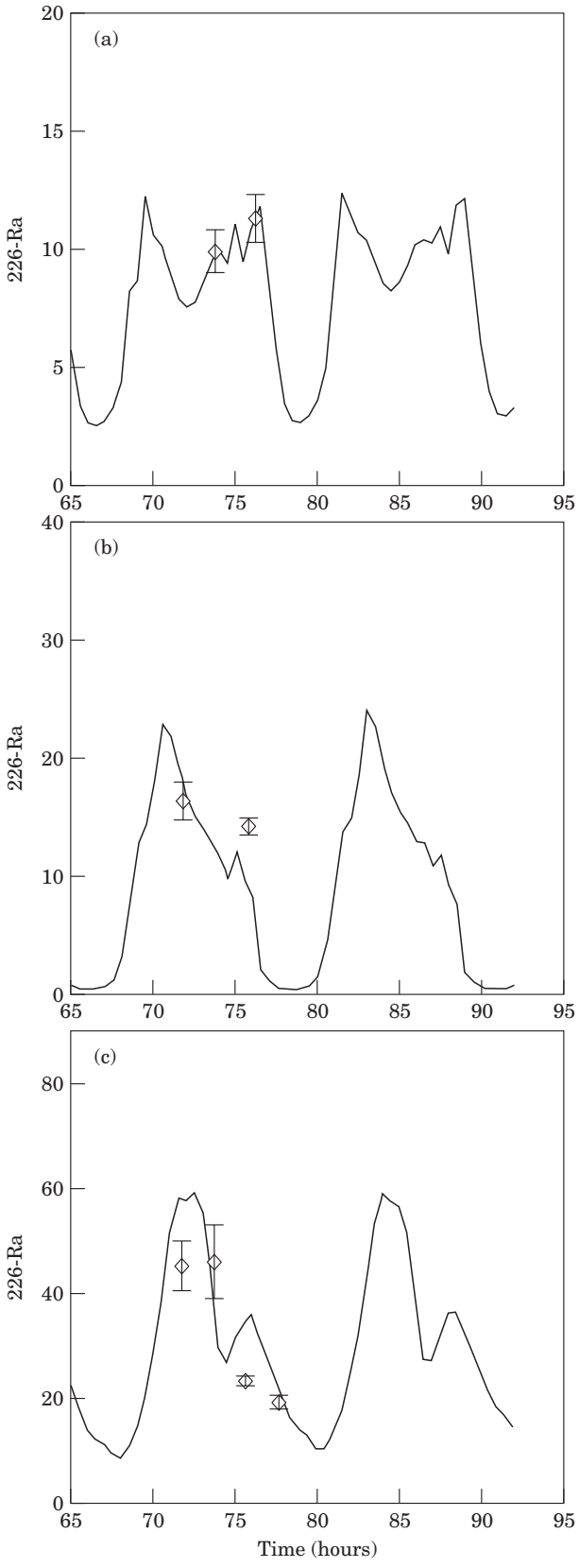


FIGURE 4. Time evolution of observed and computed $^{226}$Ra concentrations in solution (mBq l$^{-1}$) in points 9(A), 5(B) and 12(C). —— Computed; –◇– Measured.

scheme has also been used to solve the diffusion terms (Kowalick & Murty, 1993). It is considered that there is no flux of radionuclides through land boundaries. Along open boundaries, the boundary condition described in Periáñez (1998, 1999, 2000) is applied.

## Model results

Only the two main tidal constituents, $M_2$ and $S_s$, have been included. As will be shown below, this is enough to have a realistic representation of the dispersion patterns of $^{226}$Ra.

The calibration of the hydrodynamic model consisted of selecting the optimum value for the bed friction coefficient $K$. After some model runs, it was selected as $K=0{\cdot}040$ for the Tinto river and $K=0{\cdot}005$ for the rest of the estuary. With these selections, a reasonable agreement between observed and computed currents has been achieved. A comparison between observed and computed magnitude and direction of the maximum currents for several locations in the estuary is presented in Table 2 for a situation of medium tides (coefficient 74·4). Once that water circulation is reproduced by the hydrodynamic model, results are treated with standard tidal analysis to calculate the tidal constants to be used by the dispersion model to compute currents and water elevation at any position and instant of time, as commented before.

Since tidal mixing is explicitly calculated, the diffusion coefficients must be chosen with respect to the real dispersion coefficient and to that of the subgrid, required to diffuse patches which become too small to be described correctly by the grid size and the numerical scheme. Lam *et al.* (1984) gave an empirical relationship linking a given patch size to a dispersion coefficient:

$$K_D = 5 \times 10^{-4} d^{1{\cdot}2} \qquad (14)$$

where $d$ is the diameter of the patch. Considering that three grid cells are an acceptable lower limit for the smaller patches to be described by the model (Breton & Salomon, 1995; Periáñez, 2000), the present grid size corresponds to a dispersion coefficient $K_D=0{\cdot}61$ m$^2$ s$^{-1}$.

Since the dispersion model is not restricted by the CFL stability criterion, time step in the dispersion model has been increased to 30 s. However, stability conditions imposed by the dispersion equation (Kowalick & Murty, 1993) are satisfied with this value.

An example of the dispersion of an instantaneous discharge, arbitrary magnitude, of a dissolved radionuclide (thus $\chi_1=k_2=0$) carried out in the Tinto river

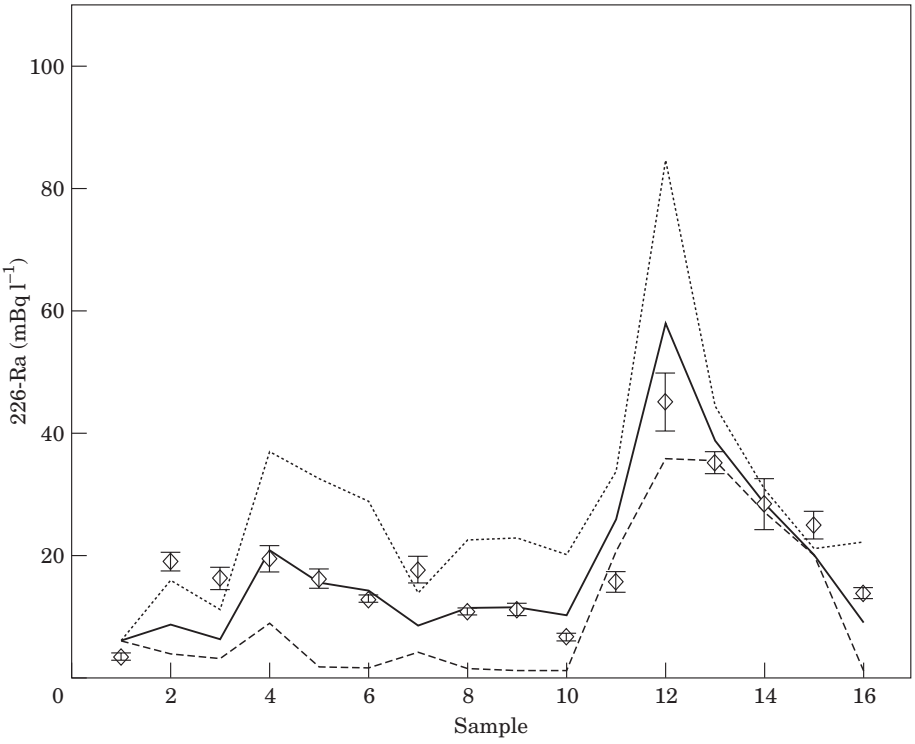


FIGURE 5. Model sensitivity to changes in parameter $\phi$. The solid line gives the model result with the selected value. —— Computed; –◇– Measured; – – – 0·01; · · · 1·0.

is presented in Figure 2. The radionuclides are released at high water, and the movement of the patch is followed during 12 h. It can be seen that the patch moves downstream the Tinto river during the ebb. During the flood, which starts approximately at 6 h, it enters the Odiel river and Canal del Burro. Indeed, previous measurements of intertidal sediments (Martínez-Aguirre & García-León, 1997) have revealed that the Canal del Burro area is also contaminated.

Some parameters must be defined to stimulate the dispersion of $^{226}$Ra including the interactions with sediments. The coefficients $\chi_1$ and $k_2$ were obtained from absorption laboratory experiments carried out with $^{133}$Ba, a $\gamma$ emitter whose chemical behaviour is very similar to that of Ra. They were carried out with unfiltered water of the Odiel estuary in such a way that laboratory conditions (temperature, pH, salinity, movement of water) were as close as possible to the natural conditions. The time increase of $^{133}$Ba activity in suspended sediments enables the coefficients to be calculated (Laissaoui *et al.*, 1998). The values obtained were $\chi_1 = 0{\cdot}55 \times 10^{-7}$ m s$^{-1}$ and $k_2 = 8{\cdot}17 \times 10^{-6}$ s$^{-1}$. The mean radius of active sediment particles is taken as $R = 15$ µm and the average bulk density of sediments as 900 kg m$^{-3}$ (Univeersidad de Sevilla, 1991). The fraction of active sediments has been taken as $f = 0{\cdot}5$ for all the estuary. Although this parameter will probably change from one position to another, the selection of a constant (but realistic) value seems enough to describe the general dispersion patterns of $^{226}$Ra. After a calibration exercise, it was selected $L = 0{\cdot}01$ m and $\phi = 0{\cdot}1$.

The model has been applied to reproduce the experimental measurements of $^{226}$Ra. An external continuous source of 667 Bq s$^{-1}$ has been considered for all the coastal cells along the Tinto river that are in contact with the phosphogypsum piles. Taking into account that there are 17 grid cells in these conditions, a total input of $1{\cdot}1 \times 10^4$ Bq s$^{-1}$ is introduced from the phosphogypsum piles. The source magnitude, since it is not independently known, has been selected by trial and error until the model gives correct activity levels. A uniform background of $^{226}$Ra in solution of 10 Bq m$^{-3}$ has been assumed to simulate the effect of previous inputs. The input from the piles is carried out over this background. The sediments of the estuary are heavily contaminated due to previous discharges from the fertilizer complex (Martínez-Aguirre *et al.*, 1994). For instance, activity in the Odiel river sediments reached 1·4 Bq g$^{-1}$. In the Tinto river sediments, activity was around 0·05 Bq g$^{-1}$. Thus, the $^{226}$Ra content in the sediments, as initial conditions for the

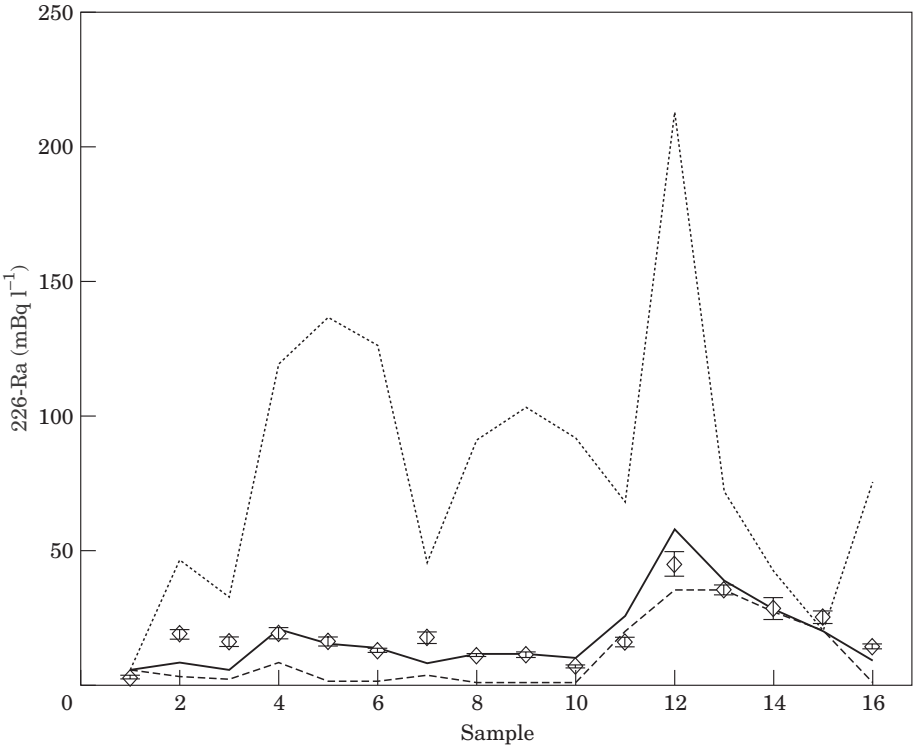


FIGURE 6. Model sensitivity to changes in parameter $L$. The solid line gives the model result with the selected value. —— Computed; –◇– Measured; – – – 0·001; · · · 0·1.

model, has been taken as 1·0 and 0·015 Bq g$^{-1}$ for the Odiel and Tinto rivers respectively.

The model computes the dispersion of $^{226}$Ra until stable oscillations in concentrations are obtained (because of tidal oscillations, a stationary situation is not reached). Results from the Tinto river and points five and 16 are obtained 2·7 days after the beginning of the simulation, time that corresponds to low water. Results for the area of the estuary extending from samples one to four are extracted 2 h later and results from the rest of the estuary 4 h later. This way, the conditions of the sampling campaign are reproduced.

A comparison between measured and computed $^{226}$Ra activity levels if presented in Figure 3. It can be seen that the model gives a realistic representation of activity levels along the estuary. The simulation has been repeated exactly in the same way but without considering interactions with the sediments. The result of this simulation is also presented in Figure 3. It seems clear that sediments are now acting as a source of $^{226}$Ra to the water column since computed activity levels are significantly lower than the measured ones if the sediment is not included in the calculations. The difference between the simulations is smaller along the Tinto river, where the input from the phosphogypsum piles is the dominant source. It seems, on the other hand, that the most important source of $^{226}$Ra to the Odiel river is redissolution from the contaminated sediment, as indicated by the difference in activity levels between the simulations. Indeed, the net input of $^{226}$Ra, for the whole estuary, from redissolution has been calculated as the difference between the redissolved and absorbed Ra, to be $2{\cdot}0 \times 10^{4}$Bq s$^{-1}$. This number is a factor of 2 larger than the input of Ra from the phosphogypsum piles (see above).

The temporal evolution (along a tidal cycle) of $^{226}$Ra concentrations at three points of the estuary (5, 9 and 12) has also been studied with the model. Results are presented in Figure 4. Although in points five and nine only two samples are available, it seems that, in general, the model gives a realistic representation of the temporal evolution of activity levels. Measurements at points five and nine suggested that there was little influence of the tidal state on activity levels in these points (see section 3). However, model results indicate that the input of water from the sea during the flood reduces $^{226}$Ra concentrations not only in point 12 (as could already be deduced from measurements), but at five and nine as well.

The model sensitivity to changes in the correction factor, $\phi$, and the mixing depth, $L$, has been investigated since these parameters were selected after model

calibration, carried out as a trial and error exercise. Results are presented in Figures 5 and 6 respectively. In general, it can be seen that these parameters affect strongly the specific activities in water. An increase in both $L$ and $\phi$ implies a higher water-sediment interaction. Thus, the redissolution process is enhanced and too high concentrations are obtained in water. The inverse effect is obtained if $L$ or $\phi$ are reduced.

## Conclusions

The presence of $^{226}$Ra in an estuary formerly affected by direct discharges from a phosphate fertilizer processing complex has been investigated. Measurements indicate that activity levels are lower than those obtained when discharges were carried out. However, the Tinto river is affected by the input of Ra from the phosphogypsum piles located by the river. Moreover, activity levels in the Odiel river are higher than those of non contaminated rivers. A numerical model of the estuary has been developed to study this hypothesis in more detail.

The model solves the 2D shallow water hydrodynamic equations for the estuary. Once calibrated, model results are treated using standard tidal analysis to calculate the tidal constants that will be read by the dispersion model to compute the instantaneous currents over the estuary. This way, faster computations can be carried out than if the hydrodynamic equations are solved simultaneously with dispersion. The dispersion model includes advection-diffusion of dissolved radionuclides plus interactions with sediments. These absorptions-desorption reactions are described in terms of kinetic transfer coefficients. Activity levels measured along the estuary can be, in general, reproduced by the model if an input of $^{226}$Ra from the phosphogypsum piles and contaminated sediments are introduced in the model. Activities detected along the Odiel river cannot be obtained with the model if sediments are not considered. This supports the idea of sediments acting as a source of pollutants, in general, to the water column once the external input of pollutants has stopped. Thus, the process of cleaning of a given estuarine environment will probably be slower than might be expected after a reduction (or cessation) of waste disposal due to the redissolution of pollutants from the contaminated sediments.

## Acknowledgements

Work supported by ENRESA, FEDER project 1FD97-0900-CO2-01 and EU contract FIGE-CT2000-00085.

## References

Aston, S. R., Assinder, D. J. & Kelly, M. 1985 Plutonium in intertidal and estuarine sediments in the northern Irish Sea. *Estuarine, Coastal and Shelf Science* **20,** 761–771.

Benes, P., Cernik, M. & Slavik, O. 1994 Modelling of migration of $^{137}$Cs accidentally released into a small river. *Journal of Environmental Radioactivity* **22,** 279–293.

Borrego, J. & Pendón, J. G. 1988 Algunos ejemplos de influencia de los procesos antrópicos en el medio sedimentario: la ría de Huelva. *Henares Rev. Geol.* **2,** 299–305 (in Spanish).

Breton, M. & Salomon, J. C. 1995 A 2D long term advection dispersion model for the Channel and southern North Sea. *Journal of Marine Systems* **6,** 495–513.

Broeker, W. S., Goddard, J. & Sarmiento, J. 1976 The distribution of Ra-226 in the Atlantic Ocean. *Earth and Planetary Science Letters* **32,** 220–235.

Cook, G. T., Mackenzie, A. B., McDonald, P. & Jones S. R. 1997 Remobilizatioin of Sellafield-derived radionuclides and transport from the northeast Irish Sea. *Journal of Environmental Radioactivity* **35,** 227–242.

Flather, R. A. & Heaps, N. S. 1975 Tidal computations for Morecambe Bay. *Geophysical Journal of the Royal Astronomical Society* **42,** 489–517.

Guimond, R. J. & Hardin, J. M. 1989 Radioactivity released from phosphate containing fertilizers and from gypsum. *Radiation and Physical Chemistry* **34,** 309–315.

Kobal, I., Brajnik, D., Kaluza, F. & Vengust, M. 1990 Radionuclides in effluent from coal mines, a coal fired power plant, and a phosphate processing plant in Zasavje, Slovenia (Yugoslavia). *Health Physics* **58,** 81–85.

Koster, H. W., Harwitz, P. A., Borger, G. W., van Weers, A. W., Hagel, P. & Nieuwenhuize, J. 1992 Po-210, Pb-210, Ra-226 in aquatic ecosystems and polders, anthropogenic sources, distribution and enhanced radiation doses in the Netherlands. *Radiation Protection Dosimetry* **45,** 715–719.

Kowalick, Z. & Murty, T. S. 1993 Numerical Modelling of Ocean Dynamics. World Scientific, Singapore, 496 pp.

Laiche, T. P. & Scott, L. M. 1991 A radiological evaluation of phosphogypsum. *Health Physics* **60,** 691–693.

Laissaoui, A., Abril, J. M., Periáñez, R., García-León, M. & García-Montaño, E. 1998 Determining kinetic transfer coefficients for radionuclides in estuarine waters: reference values for $^{133}$Ba and effects of salinity and suspended load concentrations. *Journal of Radioanalytical Nuclear Chemistry* **237,** 55–61.

Lam, D. C. L., Murthy, C. R. & Simpson, R. B. 1984 Effluent Transport and Diffusion Models for the Coastal Zone. *Lecture Notes on Coastal and Estuarine Studies*. Springer, Berlin, 356 pp.

Martínez-Aguirre, A. & García-León, M. 1997 Radioactive impact of phosphate ore processing in a wet marshland in southwestern Spain. *Journal of Environmental Radioactivity* **34,** 45–57.

Martínez-Aguirre, A., Morón, M. C. & García-León, M. 1991 Measurements of U and Ra isotopes in rainwater samples. *Journal of Radioanalytical Nuclear Chemistry.* **152,** 37–46.

Martínez-Aguirre, A., García-León, M. & Ivanovich, M. 1994 The distribution of U, Th and $^{226}$Ra derived from the phosphate fertilizer industries on an estuarine system in southwest Spain. *Journal of Environmental Radioactivity* **22,** 155–177.

Morón, M. C., García-Tenorio, R., García-Montaño, E., García-León, M. & Madurga, G. 1986 An easy method for the determination of Ra isotopes and actinide alpha emitters from the same water sample. *Applied Radiation Isotopes* **37,** 383–389.

Nyffeler, U. P., Li, Y. H. & Santschi, P. H. 1984 A kinetic approach to describe trace element distribution between particles and solution in natural aquatic systems. *Geochimica et Cosmochimica Acta* **48,** 1513–1522.

Periáñez, R. 1998 A three dimensional $\sigma$ coordinate model to simulate the dispersion of radionuclides in the marine environment: application to the Irish Sea. *Ecological Modelling* **114,** 59–70.

Periáñez, R. 1999 Three dimensional modelling of the tidal dispersion of non conservative radionuclides in the marine environment: application to $^{239,\ 240}$Pu dispersion in the eastern Irish Sea. *Journal of Marine Systems* **22,** 37–51.

Periáñez, R. 2000 Modelling the tidal dispersion of $^{137}$Cs and $^{239,240}$Pu in the English Channel. *Journal of Environmental Radioactivity* **49,** 259–277.

Periáñez, R. & García-León, M. 1993 Ra isotopes around a phosphate fertilizer complex in an estuarine system at the southwest of Spain. *Journal of Radioanalytical Nuclear Chemistry* **172,** 71–79.

Periáñez, R. & Martínez-Aguirre, A. 1997 Uranium and thorium concentrations in an estuary affected by phosphate fertilizer processing: experimental results and a modelling study. *Journal of Environmental Radioactivity* **35,** 281–304.

Periáñez, R., Abril, J. M. & García-León, M. 1996*a* Modelling the dispersion of non conservative radionuclides in tidal waters. Part 1: conceptual and mathematical model. *Journal of Environmental Radioactivity* **31,** 127–141.

Periáñez, R., Abril, J. M. & García-León, M. 1996*b* Modelling the suspended matter distribution in an estuarine system. Application to the Odiel river in southwest Spain. *Ecological Modelling* **87,** 169–179.

Puerto Autónomo de Huelva 1989 Estudio de corrientes en la ría de Huelva. Technical Report produced by INTECSA (in Spanish).

Pugh, D. T. 1987 *Tides, Surges and Mean Sea Level.* Wiley, Chichester, 472 pp.

Universidad de Sevilla 1991 Coeficientes de distribución de radionucleidos. Contract with ENRESA, Final Report (in Spanish), 114 pp.

Vested, H. J., Baretta, J. W., Ekebjærg, L. C. & Labrosse, A. 1996 Coupling of hydrodynamical transport and ecological models for 2D horizontal flow. *Journal of Marine Systems* **8,** 255–267.